

Case Report

Juvenile Granulosa Cell Tumor as the Presenting Feature of McCune-Albright Syndrome

Brynn E. Marks,^{1,2,*} Ronan Sugrue,^{3,*} Wallace Bourgeois,^{4,*}
A. Lindsay Frazier,⁴ Stephan D. Voss,⁵ Marc R. Laufer,³ Catherine M. Gordon,^{1,6}
and Laurie E. Cohen^{1,4}

¹Division of Endocrinology, Boston Children's Hospital, Boston, MA, USA; ²Division of Endocrinology, Children's National Hospital, Washington, DC, USA; ³Division of Gynecology, Boston Children's Hospital, Boston, MA, USA; ⁴Cancer and Blood Disorders Center, Dana-Farber/Boston Children's, Boston, MA, USA; ⁵Department of Radiology, Boston Children's Hospital, Boston, MA, USA; and ⁶Division of Adolescent/Young Adult Medicine, Boston Children's Hospital, Boston, MA, USA

ORCID numbers: 0000-0002-4849-9774 (B. E. Marks); 0000-0001-9379-5540 (R. Sugrue); 0000-0002-6935-8890 (W. Bourgeois); 0000-0002-6295-987X (M. R. Laufer); 0000-0001-7152-8249 (C. M. Gordon); 0000-0002-8196-8800 (L. E. Cohen).

*These authors contributed equally as co-first authors.

Received: 22 December 2020; Editorial Decision: 14 May 2021; First Published Online: 8 July 2021; Corrected and Typeset: 15 July 2021.

Abstract

Introduction: *GNAS* mutations have been reported in both McCune-Albright syndrome (MAS) and juvenile granulosa cell tumors (JGCT) but have never been reported simultaneously in the same patient.

Case Presentation: A 15-year-old girl developed secondary oligomenorrhea. Laboratory studies revealed suppressed gonadotropin levels with markedly elevated estradiol and inhibin B levels. Pelvic ultrasound showed a 12-cm heterogeneous right adnexal mass; pelvic magnetic resonance imaging to further characterize the mass displayed heterogeneous bilateral femoral bone lesions initially concerning for metastatic disease. Positron emission tomography/computed tomography showed minimal ¹⁸F-fluorodeoxyglucose (FDG) uptake in the pelvic mass but unexpectedly revealed FDG uptake throughout the skeleton, concerning for polyostotic fibrous dysplasia in the context of MAS. The adnexal mass was excised and pathology confirmed a JGCT. The patient's affected bone and JGCT tissue revealed the same pathogenic *GNAS* p.R201C mutation, while her peripheral blood contained wild-type arginine at codon 201.

Conclusion: This mutation has been previously reported in cases of MAS and JGCT but never simultaneously in the same patient. This demonstration of a *GNAS* mutation underlying both JGCT and MAS in the same patient raises questions about appropriate surveillance for patients with these conditions.

Key Words: McCune-Albright syndrome, juvenile granulosa cell tumor, fibrous dysplasia, *GNAS* gene, pediatric endocrinology

The differential diagnosis for secondary oligomenorrhea is broad. However, the etiology can often be established when following an algorithmic approach for further diagnostic testing. In this case, the patient was found to have both McCune-Albright syndrome (MAS) and a juvenile granulosa cell tumor (JGCT). MAS is characterized by mosaicism, wherein a *GNAS* mutation arising early in embryonic development causes the MAS phenotype. Somatic *GNAS* mutations are also reported in several different types of tumors, including JGCTs. This is the first report wherein a patient with MAS was found to have a JGCT with sequencing demonstrating the same *GNAS* mutation in each affected tissue. This observation introduces new challenges for long-term surveillance in patients with MAS or JGCT.

Case Report/Case Presentation

Patient Presentation

Written assent from the patient and consent from a parent to publish her case, including images, were obtained. The patient was diagnosed with overt hypothyroidism due to Hashimoto thyroiditis at age 13 years, 10 months. During routine endocrine follow-up at 14 years, 4 months of age, she reported that her menstrual periods had become irregular over the preceding 4 months, although they had previously been regular since menarche at 12 years, 8 months of age. Her review of systems was otherwise negative. Thyroid function was normal on levothyroxine replacement. After being asked to track her menses, she returned to care at 15 years, 4 months of age reporting up to 2 months without any vaginal bleeding followed by periods of heavy bleeding lasting up to 2 weeks. Family history was notable for maternal hypothyroidism but no other autoimmune conditions, infertility, or first-degree relatives with breast, ovarian, uterine, or colon cancer.

On physical examination, her height was 165.8 cm [+0.8 SD score (SDS)], her weight was 79.2 kg (+1.9 SDS), and her BMI was at the 95th percentile (+1.9 SDS). Her vital signs were normal for age, and her physical examination was normal apart from symmetric thyromegaly approximately 1.5 times normal size. She did not have any café-au-lait spots.

Laboratory and Imaging Studies

As part of her evaluation, luteinizing hormone (LH) and follicle-stimulating hormone (FSH) levels were obtained to rule out premature ovarian insufficiency but returned suppressed (see Table 1 for lab values). She was also noted to have hyperprolactinemia (56.67 ng/mL), which was consistently elevated with serial dilutions and prompted

Table 1. Laboratory values and reference ranges obtained during diagnostic work-up

	Patient's value	Reference range
Luteinizing hormone	<0.10 IU/L	Follicular: 2.1-12.2 IU/L Mid-cycle: 18.1-71.8 IU/L Luteal: 0.7-16.8 IU/L
Follicle-stimulating hormone	<0.10 IU/L	Follicular: 3.0-11.3 IU/L Mid-cycle: 4.8-34.2 IU/L Luteal: 0.9-9.7 IU/L
Prolactin	56.67 ng/mL	<26 ng/mL
Thyroid-stimulating hormone	3.310 mcunit/mL	0.7-5.7 mcunit/mL
Free thyroxine	1.13 ng/dL	0.80-1.90 ng/dL
Insulin-like growth factor-I	182.0 ng/mL	208.0-444.0 ng/mL
Free testosterone	2.6 pg/mL	1.2-7.5 pg/mL
Cortisol	19.2 mcg/dL	5.0-25.0 mcg/dL
Sex hormone binding globulin	175.7 nmol/L	11.0-120.0 nmol/L
Estradiol (immunoassay)	1074.0 pg/mL	Follicular: 30-500 pg/mL Luteal: 100-300 pg/mL
Estradiol (tandem mass spectrometry)	1030.0 pg/mL	9.0-249.0 pg/mL
Inhibin B	>4325 pg/mL	50-475 pg/mL
Beta-human chorionic gonadotropin	<0.1 mIU/mL	0-5.0 mIU/mL
Alpha fetoprotein	1.0 ng/mL	0-15.0 ng/mL
Cancer antigen 125	14 unit/mL	0-35 unit/mL

additional studies to evaluate the hypothalamic-pituitary axis. She was found to have a low insulin-like growth factor-I (IGF-I) level for age and pubertal status. A morning cortisol level was normal. A brain magnetic resonance imaging (MRI) to evaluate the hypothalamus and pituitary was normal. As part of the evaluation for polycystic ovarian disease, a free testosterone level was obtained and was normal, but sex hormone-binding globulin was markedly elevated (175.7 nmol/L). An estradiol level determined by immunoassay was 1074 pg/mL (3943 pmol/L) and then was still significantly elevated at 969 pg/mL (3558 pmol/L) when repeated by tandem mass spectrometry to rule out heterophile antibody interference. An inhibin B level was above the upper limit of the assay at >4325 pg/mL, thus raising concern for an ovarian tumor.

A pelvic ultrasound showed a heterogeneous, predominantly solid 11 × 12 × 8 cm right adnexal mass (Fig. 1A) without other abnormalities (Fig. 1B). A pelvic MRI (Fig. 1C and 1D) showed multiple heterogeneous foci of abnormal, enhancing bone marrow signal in the proximal

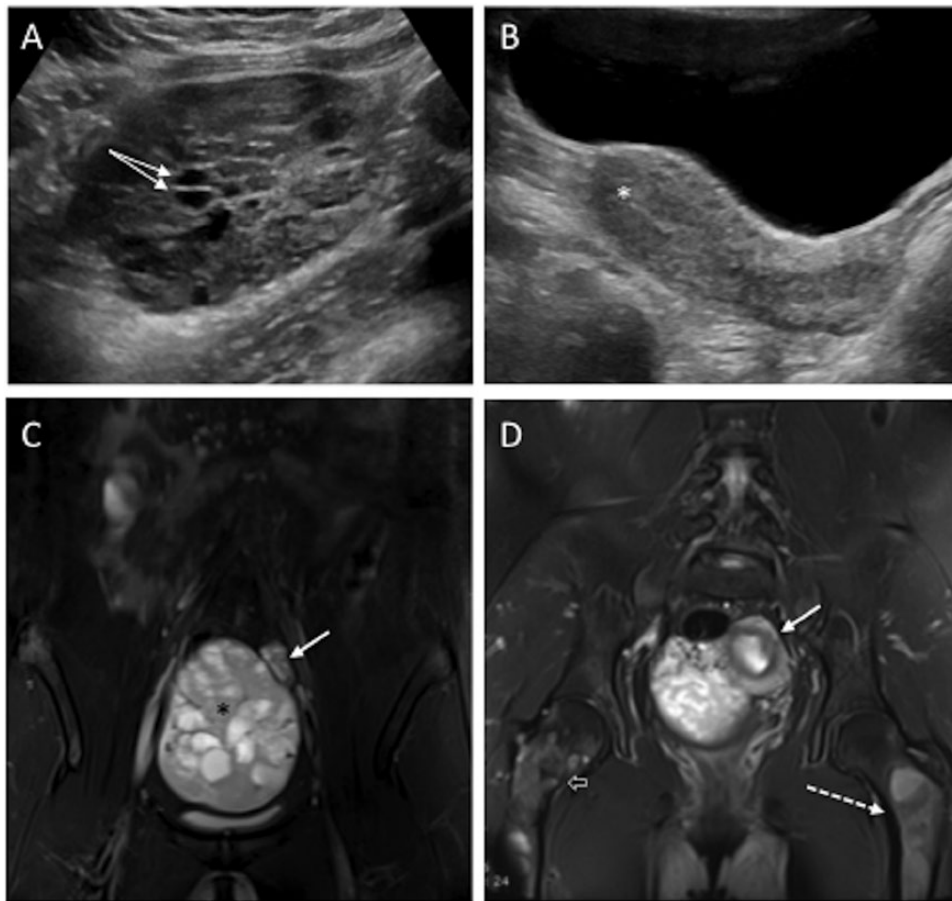


Figure 1. (A) Ultrasound image showing a heterogeneous, predominantly solid mass with scattered cystic areas (arrows). (B) Normal postpubertal sonographic appearance of the uterus and endometrium (*). (C, D) Pelvic MRI with coronal fat-suppressed T2-weighted (C) and postgadolinium enhanced fat-suppressed T1-weighted (D) images show the cystic/solid pelvic mass (*) and a normal left ovary (C, arrow) with heterogeneous enhancement and mass effect upon the uterus (D, arrow). Also evident is abnormal enhancement and expansion of the bone marrow space (D, dashed arrow) with linear disruption of the right femoral neck cortex, concerning for pathologic fracture (D, open arrow).

femurs bilaterally with expansion of the marrow space, cortical thinning, and a linear abnormality across the right femoral neck concerning for fracture (Fig. D, arrows). These lesions on MRI and radiographs (Fig. 2) were initially concerning for metastatic disease. The patient had not reported any bone pain and was physically active.

Based on these results, an ^{18}F -fluorodeoxyglucose (FDG) positron emission tomography (PET)/computed tomography was obtained for staging of a possible primary ovarian tumor with metastatic spread. The PET imaging showed intense multifocal FDG uptake throughout the axial and appendicular skeleton. The right adnexal mass showed very low level FDG uptake (Fig. 2A). Consistent with the earlier pelvic radiograph (Fig. 2B), the CT portion of the PET examination (Fig. 2C) revealed extensive osseous abnormalities characterized by expansile lytic lesions, endosteal cortical thinning, expansion of the medullary cavity, and a diffuse pattern of groundglass attenuation, all of which were associated with intense FDG uptake in a

pattern characteristic of polyostotic fibrous dysplasia. This finding suggested the possibility of MAS.

A right tibial bone biopsy was performed to further elucidate the diagnosis of fibrous dysplasia *vs* metastatic lesions. The pathology was equivocal, showing reactive bony trabeculae with focal associated osteoblasts and intervening stroma composed of bland spindle cells. This was reported as benign, although findings at the margin were suggestive of a fibro-osseous lesion secondary to fibrous dysplasia. Genetic testing from this biopsy was also sent (see following discussion).

The question arose as to whether the ovarian mass reflected ovarian hyperstimulation, a manifestation of MAS, or an ovarian tumor. Despite the low level of FDG-avidity in the ovarian mass, the large size, significant solid component, and markedly elevated inhibin B level was most suspicious for malignancy. After multidisciplinary discussion, the decision was taken to undergo primary treatment for a likely ovarian tumor via exploratory laparotomy and



Figure 2. (A) Whole body PET maximum intensity projection image from ^{18}F -fluorodeoxyglucose (FDG) positron emission tomography (PET)/computed tomography (CT) examination with intense multifocal sites of FDG uptake (arrows), including the entire right femur, right tibia, proximal left femur, right ileum, acetabula, and right forearm. Pelvic radiograph (B) and coronal thick slab minimum intensity projection CT image of the lower extremities, reconstructed from the attenuation correction CT component of the PET/CT exam (C) show lytic lesions (B, arrow), endosteal cortical thinning and expansion of the medullary cavity (dashed arrows), and a diffuse pattern of ground-glass attenuation (open arrows), all corresponding to the sites of FDG uptake on the PET scan.

surgical resection. Upon entering the peritoneal cavity, a large pelvic mass arising from the right adnexa was noted. Peritoneal fluid suspicious for mass rupture was noted and pelvic washings were sent for cytology. The fallopian tubes, left adnexa, uterus, bladder, mesentery, and peritoneum appeared normal, and no implants or lymphadenopathy were identified. Intraoperative frozen section from the mass demonstrated sheets of monotonous cells with abundant eosinophilic cytoplasm, likely of sex cord stromal origin. A right salpingo-oophorectomy was performed, and the patient underwent an uncomplicated postoperative course.

Diagnosis and Treatment

Gross examination of the right ovary demonstrated a 14.5 cm, encapsulated, lobulated, tan-white mass. The right fallopian tube appeared normal. Sections of the mass revealed focally hemorrhagic, solid and cystic, tan-yellow

surfaces with multifocal necrotic and gelatinous areas. Small cuboidal and polygonal cells with scant cytoplasm and coffee-bean nuclei were noted, consistent with a low-grade malignant neoplasm originating from granulosa cells. Immunohistochemistry of the ovarian mass was positive for inhibin, calretinin, and steroidogenic factor 1, confirming the diagnosis of a JGCT. Cytology from pelvic washings was negative, and there was no lymph node involvement. The JGCT was sent for a targeted next-generation sequencing cancer panel at Brigham and Women's Hospital that surveys exonic DNA sequences of 447 cancer genes and 191 regions across 60 genes for rearrangement. A pathogenic, Tier 1 mutation in *GNAS* c.601C>T (p.R201C variant) was found in 42% of 478 reads without other Tier 1, 2, or 3 mutations or copy number variants found. This *GNAS* mutation has previously been associated with MAS and separately with JGCT [1,2]. A bone biopsy from the right tibia was sent to Washington University in St. Louis for targeted next-generation sequencing of the *GNAS* gene, which demonstrated the same *GNAS* p.R201C variant. Peripheral blood was sent to Prevention Genetics for Sanger sequencing analysis of the *GNAS* gene and demonstrated wild-type arginine at codon 201, consistent with the mosaic distribution of this mutation.

Due to the finding of tumor rupture at the time of resection, the JGCT was classified as International Federation of Gynecology and Obstetrics Stage Ic2. While observation is recommended for International Federation of Gynecology and Obstetrics Stage Ia and Ib JGCTs that have been completely resected, Stage Ic tumors with preoperative or intraoperative rupture require systemic chemotherapy given that rupture may confer inferior outcomes [3]. As such, the patient was treated with 4 cycles of bleomycin, cisplatin, and etoposide [4,5]. At the end of therapy, the patient's inhibin B, FSH, LH, and estradiol levels normalized, and she remains in remission 16 months following therapy.

Discussion/Conclusion

MAS occurs due to somatic activating mutations in *Gsa*, the alpha subunit of the G protein coupled receptor of the *GNAS* complex located on the long arm of chromosome 20 [1]. Given the mutation arises early during embryonic development, it manifests as a mosaic phenomenon whereby the phenotype depends on which tissues have the *GNAS* mutation. MAS is typically, but not always, characterized by the triad of café-au-lait spots, fibrous dysplasia, and peripheral precocious puberty [6]. As many hormone receptors contain *Gsa*, patients with MAS can also present with variable presentation of hyperthyroidism, growth hormone-secreting pituitary adenomas, and Cushing syndrome with

variable presentation due to somatic mosaicism [7-10]. Within the bone marrow, constitutive activation of $Gs\alpha$ in the stromal cells results in fibrous dysplasia [11]. Depending on age of onset, LH receptor-activating mutations seen in girls with MAS may manifest as precocious puberty, abnormal uterine bleeding, or primary or secondary amenorrhea [12,13]. Ovarian involvement is usually asymmetric due to mosaicism and characterized by large ovarian cysts, most typically unilateral with mixed cystic and solid components. Ovarian malignancies are not a commonly recognized component of the phenotype of MAS. In one of the largest series of patients with signs of MAS, 40 of 113 patients had ovarian cysts, ovarian tissue, or fluid sampled, but none had JGCT [14].

JGCTs constitute only 5% of all pediatric ovarian tumors [14]. In adults, the gold standard for both staging and primary treatment of early-stage ovarian cancers is surgical cytoreduction with bilateral salpingo-oophorectomy, hysterectomy, and both pelvic and para-aortic lymph node dissection. In children and in adults wishing to preserve fertility, however, the optimal treatment is less clear [3,15]. In this setting, fertility-sparing surgery via resection of the affected ovary and ipsilateral fallopian tube may be appropriate [16]. As previously stated, the decision to treat with systemic chemotherapy was due to preoperative tumor rupture, which can confer inferior outcomes with observation alone [3].

Greater than 60% of JGCTs have in-frame duplications in the *AKT1* gene, which encodes for a kinase involved in ovarian mitogenic signaling [17]. Kalfa et al reported a series of 30 patients with JGCT in which 30% had mutations in codon 201 of the *GNAS* gene (arginine to cysteine or arginine to histidine). None of these patients had signs or symptoms of MAS [18]. *GNAS* mutations, particularly in codon 201, have also been identified in other tumors, including pituitary adenomas and Leydig cell tumors, as well as thyroid, adrenocortical, and colorectal carcinomas [19]. Although the role of *GNAS* mutations in tumorigenesis has not been fully elucidated, codon 201 *GNAS* mutations lead to increased activation of $Gs\alpha$, which then drives adenylyl cyclase and increased synthesis of 3',5'-cyclic adenosine 5'-monophosphate (cAMP) [20-22]. cAMP-dependent protein kinase A (PKA) is the mediator of cAMP signaling, and abnormalities in the PKA signaling pathway have been linked to tumor formation in endocrine tissues, both as a result of activating mutations in *GNAS* and inactivating mutations of regulatory subunits of PKA (*PRKAR1A* mutations in the example of the multiple neoplasia syndrome Carney complex) [23]. However, the apparent infrequency of JGCT in patients with MAS suggests that *GNAS* mutations result in relatively weak oncogenes and that ovarian stromal cells require other cooperating

mutations to initiate tumorigenesis. For example, work in other cancers has suggested that activating *GNAS* mutations can cooperate with *APC* inactivation in colorectal tumorigenesis [20] or with *KRAS* mutations in pancreatic neoplasms [24].

While *GNAS* mutations underlie both MAS and JGCT, to date there has not been a case reported wherein a patient was found to have both MAS and JGCT with analysis of both tissues showing the same *GNAS* mutation. Kalfa et al have speculated about the relationship between MAS and JGCT, calling the link between the 2 "an open question" given the mutual pathophysiological mechanism yet the absence of reported cases of a patient harboring the 2 entities [18].

Furthermore, this case highlights the impact of markedly elevated estradiol levels on other hormones. The patient's suppressed IGF-I levels were likely due to hepatic resistance to growth hormone from markedly elevated estradiol [25]. Although MAS has been associated with hyperprolactinemia due to somatotroph hyperplasia, the patient's prolactin normalized after treatment, which suggests that hyperprolactinemia was likely caused by increased estradiol binding to the estrogen response element on the prolactin genes in the lactotroph cells [26].

This case raises important questions as to the management of children with MAS or JGCT. For a patient with MAS and ovarian abnormalities, should tumor markers be assessed given their risk of developing a JGCT? Fundamentally, should these patients be considered to have a cancer-predisposition syndrome? Despite growing literature documenting *GNAS*-positive cancers of the ovary, breast, pancreas, liver, and smooth muscle, the most recent best practice management guidelines issued by the Fibrous Dysplasia/McCune-Albright International Consortium in 2019 recommend adherence to general cancer screening programs without any disease specific modifications [19,27-30]. Similarly, in a patient with a JGCT where a *GNAS* mutation is found, what should be their subsequent endocrine work-up and surveillance? Although the incidence of overlap between MAS and JGCT is rare, the findings presented here suggest that for patients diagnosed with either JGCT or MAS, investigating for the presence of the other disorder may be prudent and, in some cases, may significantly impact clinical management.

Acknowledgments

Author Contributions: BEM, RS, and WB were involved in the patient's care, drafted the initial manuscript, and reviewed and revised the manuscript. ALF, MRL, CMG, and LEC were involved in the patient's care and reviewed and revised the manuscript. SDV was involved in the patient's care, reviewed imaging studies, created figures, and reviewed and revised the manuscript. All

authors approved the final manuscript as submitted and agree to be accountable for all aspects of the work

Additional Information

Correspondence: Laurie E. Cohen, MD, Division of Endocrinology, Boston Children's Hospital, 300 Longwood Avenue, Boston, MA 02115, USA. E-mail: laurie.cohen@childrens.harvard.edu.

Disclosures: BEM has received grant funding from the Pediatric Endocrine Society, Tandem Diabetes Care, Inc., Cystic Fibrosis Foundation, and the Boston Children's Academy for Teaching and Educational Innovation and Scholarship. ALF serves on the clinical advisory board for Decibel Therapeutics. SDV received an honorarium from Springer Verlag for book editing. MRL has received grant funding from the J Williard and Alice S Marriott Foundation, the Marriott Daughters Foundation, and Department of Defense; royalties from UpToDate and Emans Laufer Goldstein's *Pediatric & Adolescent Gynecology* (7th ed., Wolters Kluwer; 2020); and advisor to Next Gen Jane and Endometriosis Association. CMG has received grant funding from the National Institutes of Health (Eunice Kennedy Shriver NICHD), the Progeria Research Foundation, and the Patty Brisben Foundation; royalties from Wolters Kluwer; serves as an Advisory Council Member for NICHD, executive committee (board of directors) Thrasher Research Fund, Subboard on Adolescent Health, American Board of Pediatrics; associate editor for Elsevier journals (*Journal of Adolescent Health and Bone*); consultant/writer for Massachusetts Medical Society (*New England Journal Watch*), Member of Data Safety and Monitoring Board, Eli Lilly, Inc. LEC has received research funding from Versartis, Ascendis, Opko, and Pfizer; honoraria for lectures authored by LEC for Schering Clinical Communications (educational grant from Novo Nordisk) and for Novo Nordisk, and for the Pediatric Endocrine Society webinar authored by LEC with educational support from Sandoz. The authors declare that they have no relevant or material financial interests that relate to the research described in this paper.

Data Availability: The data are not publicly available due to their containing clinical information that could compromise the privacy of the patient. Data sharing is not applicable.

References

- Weinstein LS, Shenker A, Gejman PV, Merino MJ, Friedman E, Spiegel AM. Activating mutations of the stimulatory G protein in the McCune-Albright syndrome. *N Engl J Med*. 1991;325(24):1688-1695.
- Shi RR, Li XF, Zhang R, Chen Y, Li TJ. GNAS mutational analysis in differentiating fibrous dysplasia and ossifying fibroma of the jaw. *Mod Pathol*. 2013;26(8):1023-1031.
- Schultz KA, Harris AK, Schneider DT, et al. Ovarian sex cord-stromal tumors. *J Oncol Pract*. 2016;12(10):940-946.
- Homesley HD, Bundy BN, Hurteau JA, Roth LM. Bleomycin, etoposide, and cisplatin combination therapy of ovarian granulosa cell tumors and other stromal malignancies: a gynecologic oncology group study. *Gynecol Oncol*. 1999;72(2):131-137.
- Pautier P, Gutierrez-Bonnaire M, Rey A, et al. Combination of bleomycin, etoposide, and cisplatin for the treatment of advanced ovarian granulosa cell tumors. *Int J Gynecol Cancer*. 2008;18(3):446-452.
- Collins MT, Singer FR, Eugster E. McCune-Albright syndrome and the extraskeletal manifestations of fibrous dysplasia. *Orphanet J Rare Dis*. 2012;7(Suppl 1):S4.
- Feuillan PP, Shawker T, Rose SR, Jones J, Jeevanram RK, Nisula BC. Thyroid abnormalities in the McCune-Albright syndrome: ultrasonography and hormonal studies. *J Clin Endocrinol Metab*. 1990;71(6):1596-1601.
- Cuttler L, Jackson JA, Saeed uz-Zafar M, Levitsky LL, Mellinger RC, Frohman LA. Hypersecretion of growth hormone and prolactin in McCune-Albright syndrome. *J Clin Endocrinol Metab*. 1989;68(6):1148-1154.
- Lee SE, Lee EH, Park H, et al. The diagnostic utility of the GNAS mutation in patients with fibrous dysplasia: meta-analysis of 168 sporadic cases. *Hum Pathol*. 2012;43(8):1234-1242.
- Mauras N, Blizzard RM. The McCune-Albright syndrome. *Acta Endocrinol Suppl (Copenh)*. 1986;279:207-217.
- Riminucci M, Collins MT, Fedarko NS, et al. FGF-23 in fibrous dysplasia of bone and its relationship to renal phosphate wasting. *J Clin Invest*. 2003;112(5):683-692.
- Pasquino AM, Pucarelli I, Passeri F, Segni M, Mancini MA, Municchi G. Progression of premature thelarche to central precocious puberty. *J Pediatr*. 1995;126(1):11-14.
- Lumbroso S, Paris F, Sultan C. Activating Gsa mutations: analysis of 113 patients with signs of McCune-Albright syndrome—a European collaborative study. *J Clin Endocrinol Metab*. 2004;89:2107-2113.
- Young RH, Dickersin GR, Scully RE. Juvenile granulosa cell tumor of the ovary. A clinicopathological analysis of 125 cases. *Am J Surg Pathol*. 1984;8(8):575-596.
- Rodriguez-Galindo C, Krailo M, Frazier L, et al; COG Rare Tumors Disease Committee. Children's oncology group's 2013 blueprint for research: rare tumors. *Pediatr Blood Cancer*. 2013;60(6):1016-1021.
- Billmire DF, Cullen JW, Rescorla FJ, et al. Surveillance after initial surgery for pediatric and adolescent girls with stage I ovarian germ cell tumors: report from the children's oncology group. *J Clin Oncol*. 2014;32(5):465-470.
- Bessière L, Todeschini AL, Auguste A, et al. A hot-spot of in-frame duplications activates the oncoprotein AKT1 in Juvenile Granulosa cell tumors. *Ebiomedicine*. 2015;2(5):421-431.
- Kalfa N, Ecochard A, Patte C, et al. Activating mutations of the stimulatory g protein in juvenile ovarian granulosa cell tumors: a new prognostic factor? *J Clin Endocrinol Metab*. 2006;91(5):1842-1847.
- Innamorati G, Wilkie TM, Kantheti HS, et al. The curious case of Gas gain-of-function in neoplasia. *BMC Cancer*. 2018;18(1):1-15.
- Wilson CH, McIntyre RE, Arends MJ, Adams DJ. The activating mutation R201C in GNAS promotes intestinal tumorigenesis in Apc(Min/+) mice through activation of Wnt and ERK1/2 MAPK pathways. *Oncogene*. 2010;29(32):4567-4575.
- Mantovani G, Lania AG, Spada A. GNAS imprinting and pituitary tumors. *Mol Cell Endocrinol*. 2010;326(1-2):15-18.
- Boussaïd K, Meduri G, Maiza JC, et al. Virilizing sclerosing-stromal tumor of the ovary in a young woman with McCune Albright syndrome: clinical, pathological, and immunohistochemical studies. *J Clin Endocrinol Metab*. 2013;98(2):E314-E320.

23. Almeida MQ, Stratakis CA. How does cAMP/protein kinase A signaling lead to tumors in the adrenal cortex and other tissues? *Mol Cell Endocrinol*. 2011;336(1-2):162-168.
24. Patra KC, Kato Y, Mizukami Y, et al. Mutant GNAS drives pancreatic tumorigenesis by inducing PKA-mediated SIK suppression and reprogramming lipid metabolism. *Nat Cell Biol*. 2018;20(7):811-822.
25. Leung KC, Johannsson G, Leong GM, Ho KK. Estrogen regulation of growth hormone action. *Endocr Rev*. 2004;25(5):693-721.
26. Murdoch FE, Byrne LM, Ariazi EA, Furlow JD, Meier DA, Gorski J. Estrogen receptor binding to DNA: affinity for nonpalindromic elements from the rat prolactin gene. *Biochemistry*. 1995;34(28):9144-9150.
27. Wong SC, Zacharin M. Long-term health outcomes of adults with McCune-Albright syndrome. *Clin Endocrinol (Oxf)*. 2017;87(5):627-634.
28. Majoor BC, Boyce AM, Bovée JV, et al. Increased risk of breast cancer at a young age in women with fibrous dysplasia. *J Bone Miner Res*. 2018;33(1):84-90.
29. Gaujoux S, Salenave S, Ronot M, et al. Hepatobiliary and pancreatic neoplasms in patients with McCune-Albright syndrome. *J Clin Endocrinol Metab*. 2014;99(1):E97-101.
30. Javaid MK, Boyce A, Appelman-Dijkstra N, et al. Correction to: best practice management guidelines for fibrous dysplasia/McCune-Albright syndrome: a consensus statement from the FD/MAS international consortium. *Orphanet J Rare Dis*. 2019;14(1):267.